# Flash Photolysis Studies of Roussin's Black Salt Anion: $Fe_4S_3(NO)_7^-$

**James Bourassa,[†] Brian Lee,[†] Stefan Bernard,[‡] Jon Schoonover,[‡] and Peter C. Ford*,[†]**

Department of Chemistry, University of California, Santa Barbara Santa Barbara, California 93106-9510, and Integrated Spectroscopy Laboratory, Los Alamos National Laboratory, Los Alamos, New Mexico 87545

*Received November 5, 1998*

A time-resolved optical (UV−vis) spectroscopic study of Roussin's black salt anion, $Fe_4S_3(NO)_7^-$, revealed two separate intermediates, **X** and **Y**, following laser flash photolysis. Both intermediates react with nitric oxide with second-order kinetics to re-form the parent complex ($k_{NO}^{X} = 1.3 \times 10^7$ $M^{-1}$ $s^{-1}$; $k_{NO}^{Y} = 7.0 \times 10^5$ $M^{-1}$ $s^{-1}$ in aqueous solutions). The shorter-lived intermediate **X** was observed in time resolved infrared spectroscopic studies. Isotopic labeling experiments involving the exchange of black salt nitrosyls with $^{15}NO_2^-$ or $^{15}N^{18}O$ were used to probe the correlation between $\nu_{NO}$ bands and the anion structures. The identities of the intermediates are interpreted in terms of photolytic loss of chemically distinct nitrosyls found on the $Fe_4S_3(NO)_7^-$ anion.

## Introduction

Previous studies have demonstrated the photolability of "Roussin's black salt" anion, $Fe_4S_3(NO)_7^-$ (RBS) toward nitric oxide release in aerated aqueous solutions.[1−3] This complex possesses many qualities desirable for the biological delivery of nitric oxide to biological targets, including water solubility, absorption across the visible light region and stability to biological conditions. Continuous wave photolysis experiments demonstrated that photolysis of the black salt in aerated solutions leads to complete fragmentation of the RBS cluster (Figure 1)[4] with a relatively small quantum yield for RBS photodecomposition ($\Phi_{RBS} = 0.0011$ for 365 nm irradiation).[1] Electrochemical detection[5] revealed that ∼6 NO's were released per cluster and eq 1 (unbalanced) summarizes the net photodecomposition products initially detected in analysis of aqueous solutions resulting from continuous photolysis experiments.[1] Nitrite and nitrate were also seen in the electrospray mass spectra of photolysis solutions. On a longer time scale (hours), ferric ion precipitates and elemental sulfur are slowly formed, but these are both apparently the result of secondary thermal processes in these aerated solutions.[1] Notably, no net photochemistry was observed in deoxygenated solutions.

$$Fe_4S_3(NO)_7^- \xrightarrow[O_2]{h\nu} 3.9Fe^{2+} + 5.9NO + 3S^{2-} + ? \quad (1)$$

Here we report flash photolysis studies of this system using time-resolved optical (TRO) and time-resolved infrared (TRIR)[6] spectroscopic techniques to probe the spectra and dynamics of possible reactive intermediates.

## Experimental Section

**Materials and Instrumentation.** Acetonitrile, dichloromethane, and 1,2-dichloroethane were distilled under dinitrogen from $CaH_2$ and used promptly. Tetrahydrofuran (THF) was distilled from sodium benzophenone ketyl solution under $N_2$. Dimethyl sulfoxide (DMSO) was distilled under reduced pressure from sodium and stored over molecular sieves. Water for spectroscopic studies was purified using a Millipore system. Methanol was distilled under dinitrogen from iodine and magnesium. Ethanol was used as received from Quantum Chemical Corporation. Argon (Air Liquide) for vacuum manifold manipulation was chromatographic grade and was first passed through an indicating oxygen trap (Chromatograph Research Supplies). Nitric oxide (Matheson, 99.0%) was passed through an Ascarite II column to remove higher nitrogen oxides.

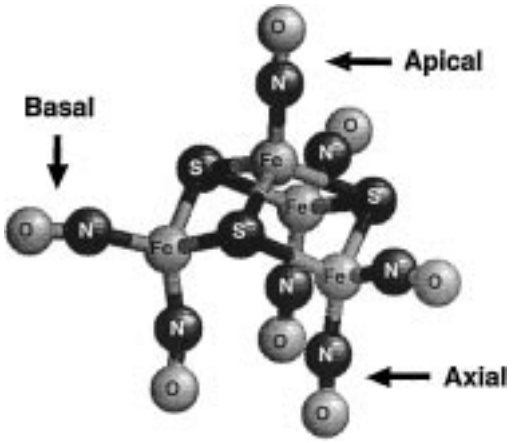


**Figure 1.** Representation of Roussin's black salt anion, $Fe_4S_3(NO)_7^-$ redrawn from coordinates reported by D'Addario et al. for $[NEt_4][Fe_4S_3(NO)_7]$ (ref 4).

The $[NH_4][Fe_4S_3(NO)_7]$ was prepared according to Seyferth et al.[7] It is stable to air in the solid form for several days, but longer-term storage should be in the dark and under inert atmosphere.

Ambient temperature IR spectra were obtained with a Bio-Rad FTS 60 FTIR spectrometer as KBr pellets or in solution cells with $CaF_2$

* To whom correspondence should be addressed.
[†] University of California, Santa Barbara.
[‡] Los Alamos National Laboratory.

(1) Bourassa, J. L.; DeGraff, W.; Kudo, S.; Wink, D. A.; Mitchell, J. B.; Ford, P. C. *J. Am. Chem. Soc.* **1997**, *119*, 2853−2861.
(2) Flitney, F. W.; Megson, I. L.; Thomson, J. L. M.; Kennovin, G. D.; Butler, A. R. *Br. J. Pharmacol.* **1996**, *117*, 1549−1557.
(3) Matthews, E. K.; Seaton, E. D.; Forsyth, M. J.; Humphrey, P. P. A. *Br. J. Pharmacol.* **1994**, *113*, 87−94.
(4) D'Addario, S.; Demartin, F.; Grossi, L.; Iapalucci, M. C.; Laschi, F.; Longoni, G.; Zanello, P. *Inorg. Chem.* **1993**, *32*, 1153−1160.
(5) Kudo, S.; Bourassa, J. L.; Boggs, S. E.; Sato, Y.; Ford, P. C. *Anal. Biochem.* **1997**, *247*, 193−202.
(6) The following abbreviations are used repeatedly in this article: RBS (Roussin's black salt anion), TRO (time resolved optical); TRIR (time resolved infrared), TB (transient bleaching), TA (transient absorption), Abs (absorbance).

10.1021/ic981282v CCC: $18.00 
Published on Web 05/21/1999

windows. Low-temperature FTIR spectra were obtained using a PFD-FT12.5 Fixed Temperature Pourfill Dewar (R. G. Hansen).[8] UV spectra were recorded with a Hewlett-Packard 8572 diode array spectrophotometer or an Olis-modified Cary 118 spectrophotometer.

**Photochemical Techniques.** UV−Vis absorption spectra and photolysis experiments under deaerated conditions were carried out in 1 cm quartz cells fitted with glass stopcocks with Viton o-ring joints. Deaeration of solutions was achieved with 3−5 freeze−pump−thaw (f-p-t) cycles. Continuous photolysis experiments were carried out using stirred solutions (3 mL) in 1 cm pathlength square quartz cells at 25 °C on optical trains using collimated light from an excitation source consisting of a 200 W high pressure short arc Hg lamp and the appropriate mercury line interference filters for wavelength isolation.[1] Chemical actinometry was performed with ferric oxalate solutions for $\lambda_{irr} < 450$ nm and with Reinecke salt solutions for longer wavelengths.

Flash photolysis experiments carried out with TRO detection apparatus used the third harmonic (355 nm) of a Nd:YAG 10 ns pulse width laser (Continuum NY60-20) attenuated to approximately 10−30 mJ/pulse as the excitation source with a beam diameter of ∼0.6 cm at the cell.[9] The probe was a high pressure short arc xenon lamp. Two detection systems were used. Kinetic traces were obtained at single monitoring wavelengths ($\lambda_{mon}$) using a SPEX Doublemate monochromator for wavelength isolation and an RCA model 8852 PMT detector. The second system recorded broad band spectra at specific delay times using an Acton Research Corp. SpectraPro-275 spectrograph and a Princeton Instruments LN2 cooled 1024EUV CCD camera.

The TRIR spectral system used in this work was designed for UV or visible flash excitation of compounds in solution with temporal IR detection in the 1550−2150 $cm^{-1}$ region.[10] Step-scan FTIR experiments were performed at Los Alamos National Laboratory using apparatus and techniques previously described.[11]

**$^{15}$N Labeling Experiments.** Solutions of PPN[$^{15}NO_2$] (20−50 mM) and C[$Fe_4S_3(NO)_7$] (0.5−2 mM; $C^+ = NBu_4^+$, $PPN^+$ ($PPN^+$ = bis(triphenylphosphoranylidene)ammonium)), $AsPh_4^+$) in dichloroethane were prepared and monitored by FTIR over the course of 24 h. Changes in the $\nu_{NO}$ region were observable after ∼1 h and were examined by spectrum subtraction. The RBS nitrosyl bands at 1800 and 1745 $cm^{-1}$ began to decrease and new bands appeared at 1786 and 1729 $cm^{-1}$ with similar relative intensities. There were no obvious changes to the band at 1706 $cm^{-1}$. Over the course of 12 h, these changes proceeded, until the new bands at 1786 and 1729 $cm^{-1}$ also began to diminish, and a second pair of $\nu_{NO}$ appeared at 1769 and 1712 $cm^{-1}$ again corresponding in relative strength and width to those originating at 1800 and 1745 $cm^{-1}$.

When a solution of RBS (200 $\mu$M) in 1,2-dichloroethane was equilibrated under 1 atm of $^{15}N^{18}O$ and transferred to an FTIR cell, the exchange of nitrosyls was noted to occur quickly. The first spectrum taken after the transfer showed that the parent nitrosyl bands had already disappeared and new bands at 1765, 1710, and 1663 $cm^{-1}$ had appeared. As the experiment progressed, the latter bands decreased in intensity while new bands grew in at 1741, 1683, and 1648 $cm^{-1}$. After 24 h, the spectrum no longer changed and was analogous to that of the original RBS solution, but with all bands shifted ∼60 $cm^{-1}$ to lower energy.

## Results and Discussion

**Spectra.** The Roussin's black salt anion is strongly colored with broad transitions across the UV−vis spectrum (Supporting Information, Figure S-1). Extinction coefficients exceed $10^3$ $M^{-1}$ $cm^{-1}$ for all $\lambda < \sim$650 nm and solutions appear black-green. Maxima appear at 270 nm ($\epsilon = 2.9 \times 10^4$ $M^{-1}$ $cm^{-1}$), 360 nm ($1.6 \times 10^4$), 420 nm ($1.02 \times 10^4$), and 550 nm ($2.6 \times 10^3$),[1] and the position and strength of these bands were not significantly affected by the solvent or identity of the counterion. Calculations at the extended Hückel molecular orbital level suggest these absorptions to be transitions between orbitals delocalized over the $Fe_4$ cluster, although the LUMO has been characterized as antibonding with respect to Fe−S and Fe−NO interactions.[4]

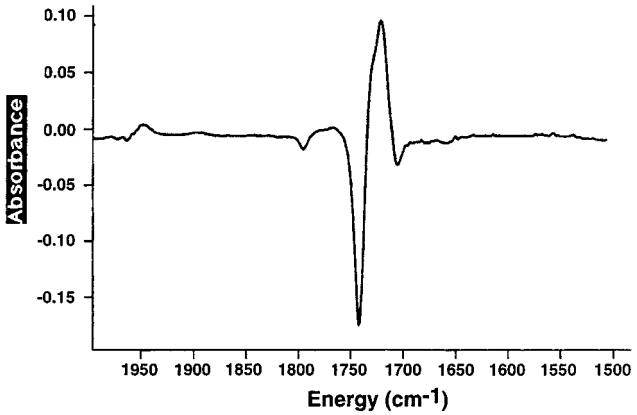


**Figure 2.** FTIR spectral changes upon photolysis of sodium RBS in 195 K THF ($\lambda_{irr} = 355$ nm). Shown is the difference spectrum relative to that of the initial spectrum before photolysis.

The sodium black salt in acetonitrile shows three bands in the nitrosyl stretching region: 1800 $cm^{-1}$ ($2.0 \times 10^3$ $M^{-1}$ $cm^{-1}$), 1745 $cm^{-1}$ ($1.2 \times 10^4$), and 1706 $cm^{-1}$ ($3.0 \times 10^3$)[1] (Supporting Information, Figure S-2). Neither positions nor relative intensities of these bands were sensitive to the cation (e.g., $K^+$, $NEt_4^+$, $AsPh_4^+$) or the solvent (methanol, THF, DMSO, or $CH_2Cl_2$). At lower temperature, these bands narrow and shift to slightly higher energies (∼3 $cm^{-1}$ at 195 K in THF). Solid state spectra taken in KBr pellets show the same bands, but that at 1745 $cm^{-1}$ is greatly broadened.

**TRIR Experiments.** Acetonitrile, methanol and THF were used as solvents in experiments to probe photolysis induced changes in the $\nu_{NO}$ region by IR spectroscopy. When aerated aqueous solutions of RBS were irradiated at ambient temperature ($\lambda_{irr} = 355$ nm), IR spectra simply showed net disappearance of the $\nu_{NO}$ bands, with no other nitrosyl peaks appearing. Photolyses of deaerated solutions led to no net spectral changes. However, at 195 K, photolyses in deaerated THF, $CH_3OH$, or $CH_3CN$ led to bleaching of the bands at 1800, 1745, and 1706 $cm^{-1}$ and concurrent appearance of a band at 1722 $cm^{-1}$ (Figure 2). This disappeared and bands characteristic of RBS returned when the samples were warmed to room temperature.

Flash photolysis with TRIR detection ($\lambda_{irr} = 355$ nm) of sodium black salt solutions in deaerated acetonitrile (0.8−1.5 mM) revealed prompt transient bleaching (TB) of the $\nu_{NO}$ band at 1745 $cm^{-1}$ and concomitant prompt transient absorption (TA) at 1720 $cm^{-1}$ consistent with spectral changes observed in the low-temperature solutions. The two signals decayed at matching rates in a few ms to values close to baseline (Supporting Information, Figure S-3). The kinetic behavior was matched by a transient bleach at the weaker RBS parent band at 1800 $cm^{-1}$, although monitoring at this frequency gave traces with greater noise. Attempts to observe absorbance changes at the weak 1706 $cm^{-1}$ band were unsuccessful due to problems with the probe source at that frequency. The magnitude and time dependencies of the traces recorded at 1720 and 1745 $cm^{-1}$ were little changed

(7) Seyferth, D.; Gallagher, M. K.; Cowie, M. *Organometallics* **1986**, *5*, 539−548.
(8) McFarlane, K. Ph.D. Dissertation, University of California, Santa Barbara, 1996.
(9) (a) Lindsay, E.; Ford, P. C. *Inorg. Chim. Acta* **1996**, *242*, 51−56. (b) Crane, D. R.; Ford, P. C. *J. Am. Chem. Soc.* **1991**, *113*, 8510−8516.
(10) (a) McFarlane, K.; Lee, B.; Bridgewater, J.; Ford, P. C. *J. Organomet. Chem.* **1998**, *554*, 49−61. (b) McFarlane, K.; Ford, P. C. *Organometallics* **1998**, *17*, 1166−1168.
(11) Schoonover, J. R.; Strouse, G. F.; Omberg, K. M.; Dyer, R. B. *Comm. Inorg. Chem.* **1996**, *18*, 165−188.

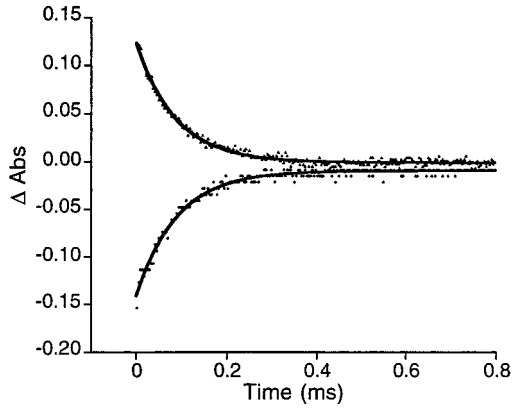


**Figure 3.** Decay of transient IR absorbance at 1720 $cm^{-1}$ and of transient IR bleach at 1745 $cm^{-1}$ observed upon flash photolysis ($\lambda_{irr}$ = 355 nm) of $CH_3CN$ solution of $Na[Fe_4S_3(NO)_7]$ (1 mM) at 296 K under 400 Torr NO. The solid curves represent the numerical fits assuming exponential decay functions. Monitoring the TA decay at 1720 $cm^{-1}$ gave $k_{obs} = 1.13 \times 10^4\ s^{-1}$; monitoring the TB decay at 1745 $cm^{-1}$ gave $k_{obs} = 1.16 \times 10^4\ s^{-1}$.

when the experiments were repeated in aerated solutions. A plot of $[\Delta Abs]^{-1}$ vs time for the regeneration of the parent 1745 $cm^{-1}$ band under Ar proved to be linear, consistent with second-order kinetics. The slope of this line is $2.74 \times 10^3\ Abs^{-1}\ s^{-1}$. If it is assumed that the flash photolysis products do not absorb appreciably at 1745 $cm^{-1}$, the known extinction coefficient of RBS can be used to estimate the second rate constant for regeneration to be $1.6 \times 10^6\ M^{-1}\ s^{-1}$.

RBS solutions under varying NO pressures displayed the same TB's and TA's in the TRIR spectra, but with increased, exponential rates of regeneration and decay. Figure 3 shows both traces for a laser flash experiment performed with a RBS solution (1 mM) in $CH_3CN$ under 400 Torr of NO. The TA at 1720 $cm^{-1}$ decayed completely to baseline; however residual bleaching, just above the noise level in the signal, remained for the parent band at 1745 $cm^{-1}$ on this time scale. Plots of $k_{obs}$ for both traces vs [NO] proved to be linear with intercepts at the origin, the slope giving the second order rate constant, $k_{NO}$, for regeneration of RBS upon reaction of the transient with NO, $k_{NO} = 2.5 \times 10^6\ M^{-1}\ s^{-1}$. Thus, the intermediate seen in the TRIR experiments occurs promptly after the laser flash, and reacts quickly with NO to reform RBS (eq 2). The $k_{NO}$ determined in this manner is considered more reliable than that derived under second-order conditions.

$$\mathbf{RBS} \underset{k_{NO}^{X}}{\overset{h\nu}{\rightleftharpoons}} \mathbf{X} + NO \qquad (2)$$

TRIR experiments with step scan FTIR detection were performed at LANL using deaerated solutions of RBS in acetonitrile and in 1,2-dichloroethane. These showed prompt formation of the TA peak at 1720 $cm^{-1}$ and of the TB at 1745 $cm^{-1}$ in a transient difference spectrum (Figure 4) very close to that recorded at low temperature (Figure 2). Both the TA and TB bands decayed over hundreds of $\mu$s.

**TRO Experiments.** Monitoring the laser flash photolysis experiment using TRO detection revealed a component of the decay kinetics not apparent in the TRIR experiments. Flash photolysis of the sodium black salt in aerated aqueous solutions (10−80 $\mu$M) with $\lambda_{mon}$ = 560 nm displayed a transient absorption that evolved (~1 ms) into a bleach that persisted for many ms. Similar traces were obtained as $\lambda_{mon}$ was tuned

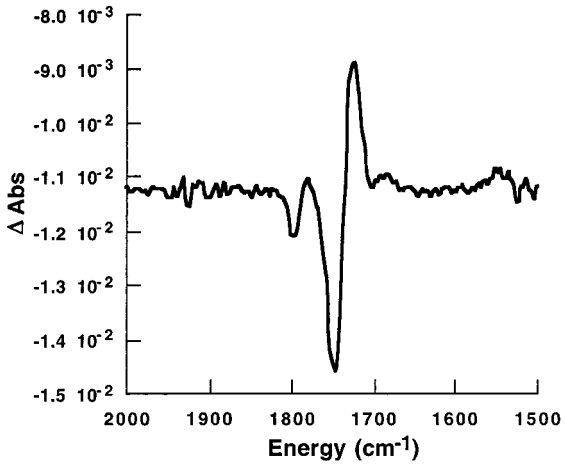


**Figure 4.** Step-scan FTIR spectrum of $[NEt_4][Fe_4S_3(NO)_7]$ (1.9 mM) solution in 1,2-dichloroethane. Delay = 50 $\mu$s, 1 $\mu$s extraction ($\lambda_{flash}$ = 355 nm).

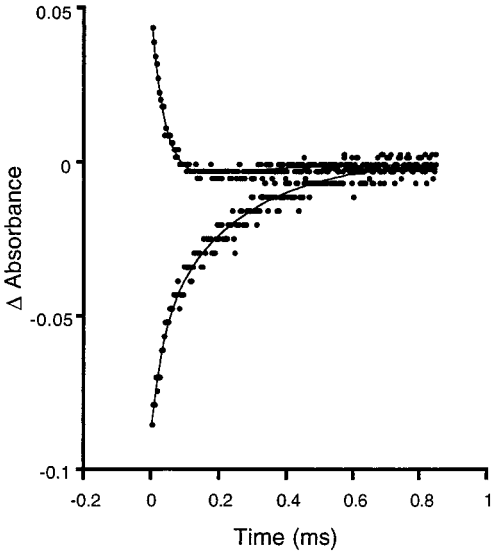


**Figure 5.** Absorption changes upon 355 nm flash photolysis of $Na[Fe_4S_3(NO)_7]$ solution (65 $\mu$M) in acetonitrile under NO (700 Torr) at 296 K (1.0 cm pathlength cell). The curve showing initial transient absorption was obtained at $\lambda_{mon}$ 560 nm and the fit shown was based on assumed simultaneous decay of two promptly formed species with $k_{obs}^{X} = 2.5 \times 10^4\ s^{-1}$ and $k_{obs}^{Y} = 0.51 \times 10^4\ s^{-1}$. The curve showing only transient bleaching was recorded at 420 nm and fit to $k_{obs}^{X} = 3.0 \times 10^4$ and $0.43 \times 10^4\ s^{-1}$.

down from 560 to 460 nm, but the magnitude of the TA component diminished until only a very weak prompt TB was seen at 460 nm. Below 460 nm, the prompt TB became more pronounced with the largest $-\Delta$Abs at 410 nm. The decay of this TB showed rates matching well with the TA decay observed at 560 nm. This did not return to baseline, but led to residual bleaching with a long lifetime ($\tau$ > 100 ms). Similar traces were obtained in acetonitrile solution. The decay of the shorter lived transient matches with that observed in the TRIR experiments. In both solvents, deoxygenation did not significantly change the traces, although it did prevent observable net photochemistry. TRO traces of the aqueous RBS solutions were not notably changed upon entraining the solutions with pure $O_2$.

Under excess NO, the decay rates for both components of the TRO traces were found to increase (Figure 5). Under such conditions, the longer lived TB seen at all wavelengths returned to baseline within the experimental time frame (100 ms). The traces at 420 nm and 560 nm both could be numerically analyzed

**Scheme 1.** Model To Analyze TRO Flash Photolysis Data of RBS Solutions

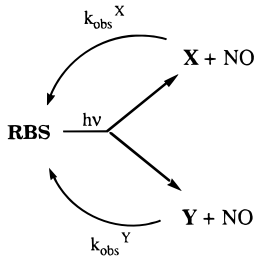


**Table 1.** Second-Order Rate Constants of the Decay of Transients Formed in the Flash Photolysis of RBS Solutions ($T = 23$ °C)

| solvent | $k_{NO}^{X}$ ($M^{-1}$ $s^{-1}$) | $k_{NO}^{Y}$ ($M^{-1}$ $s^{-1}$) | detection method |
|---|---|---|---|
| $H_2O$ | $(13 \pm 1) \times 10^6$ | $(7.0 \pm 0.6) \times 10^5$ | TRO |
| $CH_3CN$ | $(2.3 \pm 0.5) \times 10^6$ | $(3.2 \pm 0.6) \times 10^5$ | TRO |
| $CH_3CN$ | $(2.5 \pm 0.3) \times 10^6$ | | TRIR |

according to model based upon the prompt formation of two species (**X** and **Y**), each of which decay exponentially (with opposite signs at 560 nm) as illustrated in Scheme 1. For a series of such runs the residuals appear as random noise upon inspection and the addition of another exponential function did not improve quality of the numerical fit. The observed rates for the faster components at both wavelengths matched well for a given [NO] (the bleach at 560 nm was too weak to be fit to good precision, but was consistent with the slower component seen at 420 nm).

Analysis of absorbance changes at 420 nm indicated that contributions of the two components to the TB were nearly equal for all traces examined. At 560 nm, the TA proved to be consistently six times stronger than the TB. The observed rate constants $k_{obs}^{X}$ and $k_{obs}^{Y}$ each increase with NO concentration, and plots of $k_{obs}^{X}$ and $k_{obs}^{Y}$ vs [NO] are linear with intercepts at the origin (Supporting Information, Figure S-4). The slopes of these plots are the rate constants $k_{NO}^{X}$ and $k_{NO}^{Y}$ for the second order reaction of NO with **X** and **Y**, respectively, to regenerate RBS (Table 1). The results were very similar for acetonitrile solutions, and the kinetics of the faster TRO component agreed well with those for decay of the intermediate.

No effect was seen upon the traces in aqueous RBS solutions upon changing the ionic strength (up to 3 M with NaCl) or pH (buffered) between 6 and 10. The traces were also unaffected by addition of L-cysteine (10 mM), $Na_2S$ (up to 1 mM), or $NaNO_2$ (up to 100 mM).

TRO spectroscopy was also performed upon aqueous sodium RBS solutions using a CCD detector. These experiments were repeated in a variety of solvents (THF, DMSO, $CH_3CN$, acetone, methylene chloride), which gave similar TRO spectra. These agreed well with the point by point TRO spectra compiled by single wavelength detection for aqueous solutions, showing the prompt bleach at ~420 nm, an isosbestic point near 460 nm and prompt TA peaking at ~560 nm in the visible region. As the time window for the collection of the TRO profile was pushed forward over hundreds of $\mu$s, the TA diminished to baseline while the TB decreased only by approximately half. This agreed with the time traces that show the fast component (bleaching in the UV, absorption in the visible) decayed within this time period, while the slow component (TB in the UV and weak TB in the visible) persisted for many ms.

**Quantum Yields for Transient Formation.** Solutions of benzophenone in benzene were prepared with absorbances at 355 nm equal to those of sodium RBS solutions studied by flash photolysis. The well characterized formation of the benzophenone triplet state ($\phi_T = 1.0$, $\epsilon_T = 7.6 \times 10^3$ $M^{-1}$ $cm^{-1}$ at 530 nm) was then used as a standard[12] to determine laser pulse intensities in order to estimate quantum yields for formation of the intermediates seen in the TRO experiments. The lower limit for the sum $\phi_{\mathbf{X}} + \phi_{\mathbf{Y}}$ can be estimated by assuming the extinction coefficients of the intermediates to be zero at 420 nm where TB is largest, i.e.,

$$\phi_{\mathbf{Y}} + \phi_{\mathbf{X}} = \left(\frac{\Delta A_{RBS}}{\Delta\epsilon}\right)\left(\frac{\epsilon_T \phi_T}{\Delta A_T}\right) \quad (3)$$

where $\Delta A_{RBS}$ is the absorbance change for the RBS sample at a given wavelength, $\Delta A_T$ is the absorbance measured from the benzophenone sample at 530 nm, and $\Delta\epsilon$ is assumed to be equal to the molar absorption coefficient of the sodium RBS salt. This gives a lower limit of $0.062 \pm 0.004$ for the combined quantum yields $\phi_{\mathbf{X}} + \phi_{\mathbf{Y}}$. Since the TB for the slower component is about half the total bleach at 420 nm, this suggests a lower limit of ~0.03 for $\phi_{\mathbf{Y}}$.

Alternatively, the quantum yield for formation of a bleached transient can be estimated by assuming the pulse intensity to be sufficient to excite all molecules in the sample volume molecule and that the bleaching of the absorption band is proportional to the quantum yield for disappearance of reactant. The latter assumption is based on the approximation that the intermediates formed do not absorb at $\lambda_{mon}$, an assumption that has a better chance of being valid for the TRIR than for the TRO experiment given that IR transitions tend to be more structure specific. In this manner, 0.2 was estimated as the quantum yield for prompt disappearance of RBS from the transient bleaching of the parent $\nu_{NO}$ band at 1745 $cm^{-1}$. This is ~3-fold larger than the $\phi_{\mathbf{X}} + \phi_{\mathbf{Y}}$ sum estimated from the TRO experiment (0.062). We suggest that the true value lies between these limits. For the TRO experiment, where we were able to measure light absorption accurately, the assumed $\Delta\epsilon$ was too large since the products probably absorb at the monitoring wavelength owing to the broad and overlapping character of the electronic transitions. This would tend to give a low value for $\phi_{\mathbf{X}} + \phi_{\mathbf{Y}}$. On the other hand, the small sample volumes and relatively high pulse intensities in the TRIR experiment would likely lead to multiple, sequential absorption of photons by RBS, thus leading to excessive estimates of the quantum yield in that case. However, regardless of the exact value of $\phi_{\mathbf{X}} + \phi_{\mathbf{Y}}$, there is no question that these estimates are nearly two orders of magnitude higher than the $\Phi_{RBS}$ determined under continuous photolysis conditions. Thus, most (>95%) of the NO released upon photoexcitation must back-react with **X** or **Y** to re-form RBS.

**Intensity Effects on Continuous Photolysis Quantum Yields.** The small quantum yields for net RBS photodecomposition under continuous photolysis in aerated media relative to yields for formation of transients indicate that competing processes control the eventual fates of the intermediates formed. In the mechanistic model proposed below, net RBS decomposition is the result of $O_2$ trapping of intermediates formed by NO photolabilization in competition with the back reaction with NO. Thus, under continuous photolysis, $\Phi_{RBS}$ should increase at higher $[O_2]$ as reported previously.[1] However, the back-reaction appears to be the dominant pathway for decay of the intermediates formed, even under continuous photolysis. Therefore, at constant $[O_2]$, the relative importance of back reaction should

(12) Hoshino, M.; Konishi, R.; Tezuka, N.; Ueno, I.; Seki, H. *J. Phys. Chem.* **1996**, *100*, 13569−13574.

**Table 2.** Quantum Yields for RBS Photodecomposition as a Function of Light Intensity in Aqueous Solution

| $I_a$ (ein $s^{-1}$ $L^{-1}$) ($\times 10^6$)[a] | $\Phi_{RBS}$ ($\times 10^3$)[b] | $\Phi_{RBS} \times I_a^{1/2}$ ($\times 10^6$) |
|---|---|---|
| $0.45 \pm 0.01$ | $2.2 \pm 0.3$ | $1.5 \pm 0.2$ |
| $3.34 \pm 0.05$ | $1.1 \pm 0.1$ | $2.0 \pm 0.2$ |
| $9.9 \pm 0.2$ | $0.68 \pm 0.04$ | $2.1 \pm 0.2$ |

[a] $I_a$ is the intensity of 365 nm light absorbed by RBS. [b] $\Phi_{RBS}$ defined as moles of RBS decomposed per einstein of light absorbed.

increase as the intensity ($I_0$) of the continuous photolysis light flux is increased since the "steady state" [NO] is a function of the rate of light absorption ($I_a$). Correspondingly, quantum yields for net product formation should decrease with increasing irradiation intensities. This phenomenon was indeed observed (Table 2).

**A Proposed Mechanism.** A mechanistic scheme must be consistent with the following observations. (i) The quantum yield for the net decomposition is very low (0.0011 in water, 0.0039 in $CH_3CN$, with $I_a = 3 \times 10^{-6}$ einsteins $L^{-1}$ $s^{-1}$ at 365 nm) in aerated solutions and is roughly proportional to the dioxygen concentration ($\Phi_{PBS}$ values of $< 10^{-6}$, 0.0011, and 0.0042 have been determined in deaerated, aerated, and oxygenated aqueous solutions, respectively).[1] (ii) Values of $\Phi_{RBS}$ are inversely related to the irradiation intensity, but not linearly so. (iii) TRO experiments reveal two different intermediates, designated **X** and **Y**, each of which is formed promptly and displays decay kinetics first order in [NO]. (iv) In the absence of $O_2$, **X** and **Y** are formed, but no net photochemistry is observed. (v) In low-temperature photolyses and step-scan FTIR experiments, a transient $\nu_{NO}$ band at 1720 $cm^{-1}$ is observed, which is apparently due to the shorter lived intermediate **X**. At ambient *T*, decay of this TA mirrors the recovery of the RBS $\nu_{NO}$ bands at 1800 and 1745 $cm^{-1}$. (vi) The total quantum yield for **X** and **Y** formation upon flash photolysis $\phi_{\mathbf{X}} + \phi_{\mathbf{Y}}$ is much higher than the net quantum yield for RBS decomposition $\Phi_{RBS}$. We will discuss these observations in the context of the reactions suggested in Scheme 2.

Since the oxygen-dependent rates are small relative to the back reaction rates, it is reasonable to take the steady state approximation for the concentrations of **X** and **Y** according to Scheme 2:

$$[\mathbf{X}]_{SS} = \frac{\phi_{\mathbf{X}} I_a}{k_{NO}^{\mathbf{X}}[NO]}, [\mathbf{Y}]_{SS} = \frac{\phi_{\mathbf{Y}} I_a}{k_{NO}^{\mathbf{Y}}[NO]} \quad (4)$$

where $\phi_{\mathbf{X}}$ and $\phi_{\mathbf{Y}}$ are the quantum yields for the photochemical formation of **X** and **Y** and $I_a$ is the flux of photons absorbed by RBS, expressed in einsteins $s^{-1}$ $L^{-1}$. If it is assumed that the steady state concentration of NO is approximately the sum of $[\mathbf{X}]_{SS}$ and $[\mathbf{Y}]_{SS}$, this gives

$$[NO]_{SS} = I_a^{1/2} \sqrt{\frac{\phi_{\mathbf{X}}}{k_{NO}^{\mathbf{X}}} + \frac{\phi_{\mathbf{Y}}}{k_{NO}^{\mathbf{Y}}}} \quad (5)$$

Accordingly, the steady state concentrations of **X**, **Y**, and NO should each be proportional to $I_a^{1/2}$.

Net photoreaction resulting from direct reaction of $O_2$ with **X** and/or **Y** according to Scheme 2 would give the following expression for the quantum yield for RBS decomposition:

$$\Phi_{RBS} = \frac{\phi_{\mathbf{X}} k_{\mathbf{X}}[O_2]}{k_{\mathbf{X}}[O_2] + k_{NO}^{\mathbf{X}}[NO]_{SS}} + \frac{\phi_{\mathbf{Y}} k_{\mathbf{Y}}[O_2]}{k_{\mathbf{Y}}[O_2] + k_{NO}^{\mathbf{Y}}[NO]_{SS}} \quad (6)$$

**Scheme 2.** Model for RBS Photochemistry

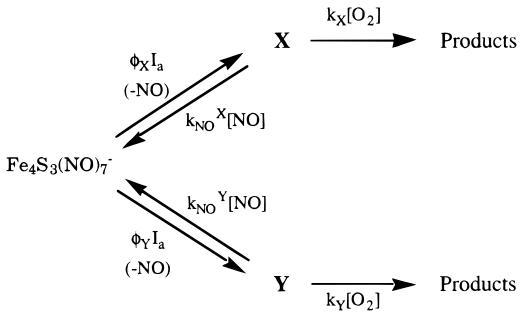


Since the back-reactions of **X** and **Y** with NO are much faster than the reactions with $O_2$, this can be simplified to

$$\Phi_{RBS} = \left(\frac{\phi_{\mathbf{X}} k_{\mathbf{X}}}{k_{NO}^{\mathbf{X}}} + \frac{\phi_{\mathbf{Y}} k_{\mathbf{Y}}}{k_{NO}^{\mathbf{Y}}}\right)\frac{[O_2]}{[NO]_{SS}} \quad (7)$$

Combining this expression with that for steady state concentration of NO (eq 5), argues that according to Scheme 2, $\Phi_{RBS}$ should be directly dependent on $[O_2]$ and inversely proportional to $I_a^{1/2}$. Although several key approximations were necessary to reach this point, it is reassuring to note that $\Phi_{RBS}$ is four times higher in oxygenated (1 atm) than in aerated aqueous solution and that the $I_a^{-1/2}$ proportionality is reasonably behaved (Table 2).

An alternative pathway leading to net photoreaction might be the trapping of NO with dioxygen (eq 8) for which the rate expression shown in eq 9 has been demonstrated.[13]

$$4NO + O_2 + 2H_2O \xrightarrow{k_{aq}} 4NO_2^- + 4H^+ \quad (8)$$

$$\frac{d[NO_2^-]}{dt} = k_{aq}[NO]^2[O_2],\ k_{aq} = 8.0 \times 10^6\ M^{-2}\ s^{-1} \quad (9)$$

If NO autoxidation were the rate-limiting process leading to RBS photodecomposition, the above rate law and the steady state expression for NO (eq 5) could be used to derive the following relationship for $\Phi_{RBS}$:

$$\Phi_{RBS} = \frac{\frac{d[NO_2^-]}{dt}}{I_a} = \frac{k_{aq}[NO]^2[O_2]}{I_a} = \frac{k_{aq}[O_2]\phi_{\mathbf{X}}}{k_{NO}^{\mathbf{X}}} + \frac{k_{aq}[O_2]\phi_{\mathbf{Y}}}{k_{NO}^{\mathbf{Y}}} \quad (10)$$

From the rate constants $k_{aq}$, $k_{NO}^{\mathbf{X}}$, and $k_{NO}^{\mathbf{Y}}$ and the solubility of $O_2$, eq 10 gives numerical values of $(1.7 \times 10^{-4} \times \phi_{\mathbf{X}}) + (3.1 \times 10^{-3} \times \phi_{\mathbf{Y}})$ for the last terms on the right in aerated solution. Given the estimated values of $\phi_{\mathbf{X}}$ and $\phi_{\mathbf{Y}}$ described above, this pathway may be numerically within an order of magnitude of the quantum yield for RBS net photodecomposition in aerated solution. Such a mechanism would be consistent with the oxygen concentration dependence of $\Phi_{RBS}$; however, eq 10 predicts no dependence upon $I_a$. Thus, NO autoxidation can not be the principal redox trapping pathway under the conditions studied here. Furthermore, it is notable that NO is sufficiently long lived in aerated solution to be detected quantitatively by electrochemical methods.[5] At sufficiently high photon flux, NO autoxidation should eventually overtake any

(13) (a) Wink, D. A.; Darbyshire, J. F.; Nims, R. W.; Saavedra, J. E.; Ford, P. C. *Chem. Res. Toxicol.* **1993**, *6*, 23−27. (b) Ford, P. C.; Wink, D. A.; Stanbury, D. M. *FEBS Lett.* **1993**, *326*, 1−3.

direct reactions of $O_2$ with **X** and **Y** (owing to the $[NO]^2$ dependence of this process) and become independent of $I_o$. However, at the highest light intensities used here, this condition was not reached.

We thus conclude that the photochemical release of NO by Roussin's black salt follows Scheme 2 where disintegration of the RBS tetranuclear framework is apparently triggered by the oxidative trapping of **X** and **Y**. This is in keeping with the electrochemistry of RBS which shows an irreversible oxidation wave leading to structural disintegration.[14]

**What Are the Identities of X and Y?** The long lifetimes and reactivity patterns clearly indicate that these are intermediates, not electronic excited states. Flash induced changes in the UV−vis absorption spectrum are featureless and not diagnostic of any particular species; however, the kinetics behaviors suggest that both species are formed by the photolabilization of NO from RBS and have the apparent stoichiometry $Fe_4S_3(NO)_6^-$. Furthermore the different reactivities of these two species toward NO indicate that they do not readily interconvert on the timescale of these experiments.

The TRIR spectrum of **X** shows a strong, new nitrosyl stretch at 1720 $cm^{-1}$ that decays with a lifetime corresponding well with those of the reappearance of the $\nu_{NO}$ at 1745 and 1800 $cm^{-1}$. The low temperature photolysis showed the 1706 $cm^{-1}$ band of RBS to be bleached in roughly the same proportions as the other $\nu_{NO}$ bands, but changes at this frequency were too small to follow by TRIR. On the other hand, no other new $\nu_{NO}$ bands were observed that could be assigned to **Y**.

To our knowledge, the IR spectrum of RBS has not been assigned. If coupling of the NO oscillators on the four iron atoms is assumed, symmetry analysis of the $\sim C_{3v}$ RBS predicts five IR active nitrosyl stretches, $3A_1$ and 2E. That only 3 $\nu_{NO}$ bands are seen could be the result of fortuitous overlapping of transitions with similar energies. Alternatively, coupling between nitrosyls on different metal centers might be quite weak. If so, three $\nu_{NO}$ bands would be predicted, one for the apical nitrosyl, and two bands from the symmetric and asymmetric coupling of the two NO's on each basal iron (Figure 1).

In order to evaluate this assignment, isotopic exchange reactions between RBS and $^{15}NO_2^-$ were initiated. NMR studies by earlier workers have demonstrated that similar reactions led to exchange only of the basal iron nitrosyls.[15] The $^{15}NO_2^-$ exchange reactions in 1,2-dichloroethane described in the Experimental Section are consistent with assigning the RBS bands at 1800 and 1745 $cm^{-1}$ as the latter vibrations. Upon reaction with $^{15}NO_2^-$, these $\nu_{NO}$ shift first to distinct intermediate positions (1786 and 1729 $cm^{-1}$) then to (1769 and 1712 $cm^{-1}$) after full isotopic exchange. The 1706 $cm^{-1}$ band showed no clear bleaching, so one may assign the 1800 and 1745 $cm^{-1}$ bands as suggested and that at 1706 $cm^{-1}$ to the $\nu_{NO}$ for the apical nitrosyl. In contrast, the exchange of $^{15}N^{18}O$ with RBS in 1,2-dichloroethane led to shifts in all three $\nu_{NO}$ bands to lower frequencies (1741, 1710, and 1663 $cm^{-1}$).[16]

In this context, we assign the intermediate **X** to be the product of NO photodissociation from one of the $Fe(NO)_2$ units. This would result in a $Fe_b$ with a single nitrosyl, hence the new $\nu_{NO}$ at 1720 $cm^{-1}$, and bleaching of those at 1800 and 1745 $cm^{-1}$. **Y** can then be assigned as the product of photodissociation of the apical nitrosyl. If so, **Y** would not be expected to display new nitrosyl bands in the TRIR experiment since shifts in the $Fe_b$ nitrosyl bands might be undetectable.[17] It is notable that the lower temperature IR experiments were able to demonstrate bleaching of the 1706 $cm^{-1}$ in amounts compatible with the expected yield of **Y** under these conditions.

In summary, TRO spectroscopy has revealed that upon photolysis of Roussin's black salt at least two intermediates, **X** and **Y**, are formed, both apparently by reversible loss of a single nitrosyl. The low quantum yield for net photochemical decomposition of RBS, and therefore for the production of NO, is due to the efficient back-reactions **X** and **Y** with NO. These intermediates are proposed to result from NO loss from a basal or the apical iron, respectively. Net photochemical decomposition of RBS is concluded to be the result of oxidative trapping of **X** and **Y** by $O_2$ followed by further redox processes of later intermediates to bring about complete destruction of the Fe−S−NO framework.

**Acknowledgment.** This work was supported by the National Science Foundation (CHE 9400919 and CHE 9726889) and by a Collaborative UC/Los Alamos Research (CULAR) Initiative grant from Los Alamos National Laboratory. TRO experiments were carried out on systems constructed with instrumentation grants from the U.S. Department of Energy University Research Instrumentation Grant Program (No. DE-FG-05-91ER79039) and from the National Science Foundation. S.B. thanks the Swiss National Science Foundation for a Postdoctoral Fellowship.

IC981282V

(14) Crayston, J. A.; Glidewell, C.; Lambert, R. J. *Polyhedron* **1990**, *9*, 1741−1746.

(15) (a) Butler, A. R.; Glidewell, C.; Johnson, I. L. *Polyhedron* **1987**, *6*, 2091−2094. (b) Butler, A. R.; Glidewell, C.; Hyde, A. R.; McGinnis, J. *Inorg. Chem.* **1985**, *24*, 2931−2934.

(16) There is an ambiguity introduced by the reactions of RBS with $^{15}N^{18}O$ in acetonitrile. The reaction was quite quick all three bands shifted, first to 1765, 1710, and 1663 $cm^{-1}$ then to 1741, 1683, and 1648 $cm^{-1}$. The shifts seen for the two higher frequency bands are consistent with the $^{15}N^{18}O$ label, the intermediate position representing exchange of one of the two $Fe_b$ nitrosyls. However, it is not clear why an intermediate position is seen for the lowest frequency $\nu_{NO}$ of the parent. If the $Fe_a$ and $Fe_b$ nitrosyls are but weakly coupled, then we would expect only two $\nu_{NO}$(apical) frequencies, one for normal NO in that site, the other with double-labeled $^{15}N^{18}O$ in that site.

(17) One might speculate that the residual bleaching seen after decay of the bleached parent IR band at 1745 $cm^{-1}$ in Figure 3 may reflect minor perturbations of that absorption as the result of NO dissociation from the apical ion to form **Y**.